

Symmetric and unsymmetric donor functionalization. comparing structural and spectral benefits of chromophores for dye-sensitized solar cells†

Daniel P. Hagberg,^a Xiao Jiang,^b Erik Gabrielsson,^a Mats Linder,^c Tannia Marinado,^b Tore Brinck,^c Anders Hagfeldt^{bd} and Licheng Sun^{*a}

Received 10th June 2009, Accepted 31st July 2009

First published as an Advance Article on the web 24th August 2009

DOI: 10.1039/b911397p

A series of organic chromophores have been synthesized in order to investigate the benefits of structural *versus* spectral properties as well as the absorption properties and solar cell performance with unsymmetrically introduced substituents in the chromophore. Exceptionally high open-circuit voltage, V_{oc} , was found for the symmetrical structurally benefited dye, which also gave the best overall solar cell performance.

Introduction

The demand for alternative power sources has drawn attention to a variety of light-harvesting devices. Among these, dye-sensitized solar cells (DSCs)¹ have attracted a large number of research groups in recent decades. So far, the conventional ruthenium-based sensitizers such as N3/N719^{2,3} and black dye⁴ have reached the promising solar-energy-to-electricity conversion efficiencies of 11% under AM 1.5 irradiation. In comparison, organic sensitizers have reached efficiencies of 6–9.8%.^{5–19} However, organic chromophores for DSCs exhibiting high molar extinction coefficients, can be prepared and easily modified and are environmentally friendly. The high extinction coefficients are needed in solid-state devices where limitation of the photovoltaic performance by low hole mobility and insufficient pore filling requires thin TiO₂ films.²⁰ Organic chromophores based on triphenylamine (TPA) donors have proved potent sensitizers in DSCs over the past few years.^{10,11,17–19,21,22} Many research groups focus on broadening the absorption spectra of the chromophores in order to increase their efficiency. The spectral red-shift of organic sensitizers is frequently associated with parallel limitations; firstly, expanding the absorption by increasing the conjugation can result in sensitization problems often referred to as aggregation,^{23–25} secondly, decreasing the HOMO–LUMO gap can result in driving force limitations for the injection and regeneration.²⁶ One principal difference between organic and Ru-based chromophores is that the main absorption band in the organic dye arises mainly due to a single, strong HOMO →

LUMO excitation, while the panchromatic absorbance of common Ru-dyes is due to numerous weakly allowed transitions. The HOMO-1 energy of organic dyes is generally too low to make any significant contribution except in the near-UV region. Moreover, it has proven difficult to absorb the near-IR photons by extending the π -conjugation of the molecule, without negatively affecting the stability and overall efficiency.²³ Given these limitations, it remains a challenge for organic sensitizers to compete with the high incident photon-to-current conversion efficiency (IPCE) of *e.g.* N719.²

In recent years a number of chromophores with insulating alkyl groups, both on the linker and the donor, have been published.^{11,19} It has been shown that the efficiencies of the sensitizers are strongly dependent on the position of these insulating groups. Hara and co-workers have elegantly elucidated the influence of the position/number of alkyl chains on the open-circuit voltage, V_{oc} , and hence the efficiency of the sensitizers.⁶ Moreover, it is well-established that electron-donating groups at the *para*-position of the TPA phenyls, *e.g.* amine or alkoxy groups, red-shift the absorption spectrum and increase efficiency, where the degree of red-shift is dependent on the electron-donating strength of the substituents.^{11,17} Tian *et al.* reported a series of chromophores with aryl amines at the *para*-position of the TPA moiety and they indeed shifted the spectra bathochromically.¹⁴ One drawback with this strategy however, is the risk of raising the HOMO potential too high, hence not matching the redox potential of the electrolyte.

We have designed and synthesized a series of chromophores based on the TPA donor group (Fig. 1). The TPA group has been substituted in the *para*-position with additional phenyl groups,

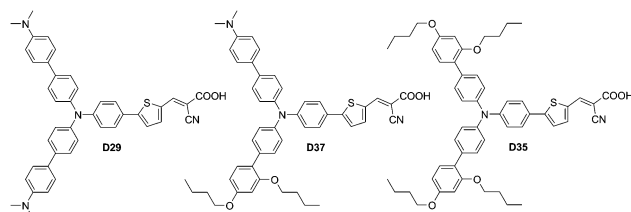


Fig. 1 Structures of the chromophores.

^aOrganic Chemistry, Center of Molecular Devices, Department of Chemistry, KTH Chemical Science and Engineering, 10044 Stockholm, Sweden

^bInorganic Chemistry, Center of Molecular Devices, Department of Chemistry, KTH Chemical Science and Engineering, 10044 Stockholm, Sweden

^cPhysical Chemistry, Center of Molecular Devices, Department of Chemistry, KTH Chemical Science and Engineering, 10044 Stockholm, Sweden

^dDepartment of Physical and Analytical Chemistry, Uppsala University, Box 259, 75105 Uppsala, Sweden

† Electronic supplementary information (ESI) available: ¹H NMR and ¹³C NMR spectra for the new compounds described in this paper, complete ref. 29 and molecular coordinates. See DOI: 10.1039/b911397p

functionalized with *p*-dimethylamine (**D29**) and/or *p,o*-butoxy groups (**D35**, **D37**). This series can be used to study the impact of structural *versus* spectral benefits on the overall solar cell efficiency. The chromophore **D29**, with dimethylaniline substituents can be regarded as a chromophore with spectral benefits, due to the strong electron-donating properties of the amine groups.

The chromophore **D35**, on the other hand, receives structural benefits from the large steric bulk introduced by the four butoxy groups, but it is not red-shifted as much as **D29**, due to lower electron-donating strength. The chromophore **D37** is a hybrid of the two parent chromophores **D29** and **D35**, and is included since it encompasses a combination of properties that might be optimal for solar cell performance. To the best of our knowledge, this is the first time such an unsymmetric organic chromophore has been presented, however, unsymmetric squaraine dyes have been investigated.²⁷ Moreover, breaking the symmetry of the molecule gives rise to orbital rearrangements. As has been observed in a different class of dyes, two explicit acceptor groups give two near-degenerate LUMOs.²⁸

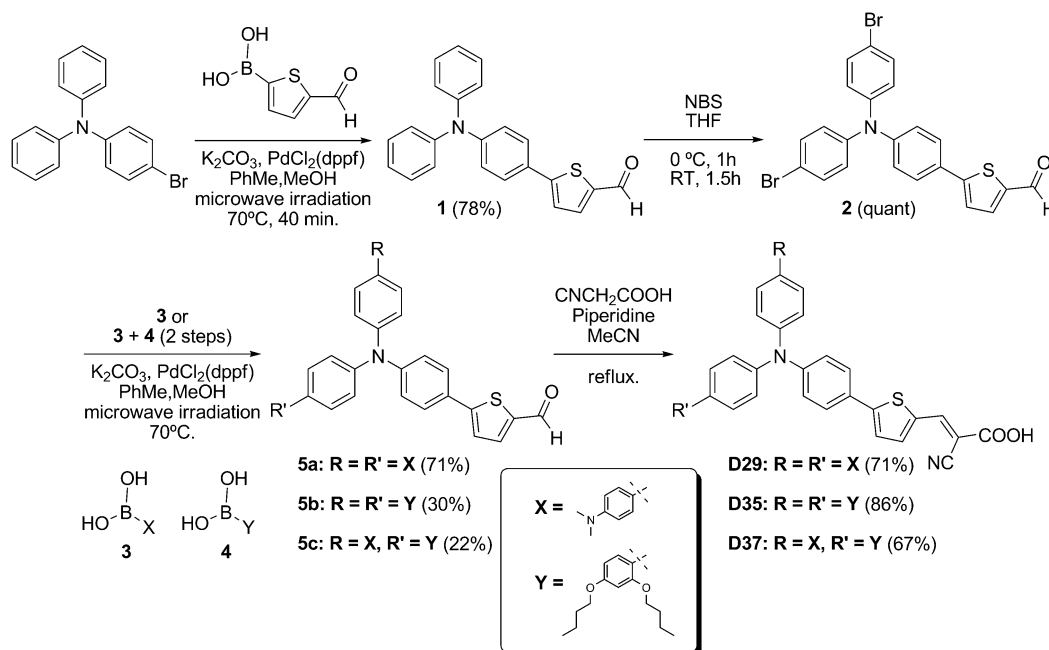
Prior to the synthesis of the three novel organic chromophores (Scheme 1), their electronic and spectral properties were evaluated using hybrid-DFT computational methods. Gas-phase optimized geometries and absorption spectra were obtained at the B3LYP/6-31G(*d*) level, employing the Gaussian03 program package.²⁹ Time-dependent DFT was used to obtain the vertical transitions. Although it is well-known that hybrid-DFT gravely underestimates the charge-transfer excitations,³⁰ present in all organic sensitizers, B3LYP does successfully reproduce the general characteristics of the spectra, making it the method of choice in this study. Fig. 3 displays the simulated absorption spectra together with the relative energy levels of the three dyes. The calculations indicate that the unsymmetric dye **D37** has more evenly spaced occupied frontier orbitals, having contributions from both the **D29** and **D35** electronic structures. The main

absorption band is predicted to be broadened at the blue end, because of a larger contribution from the HOMO-1 → LUMO transition, which is essentially forbidden in **D29** and **D35**. This difference is mainly due to a better overlap between HOMO-1 and LUMO in **D37** (Fig. 2). The calculations predict a systematic red-shift, when increasing the number of dimethyl amines in the functional groups.

Results and discussion

The straightforward synthesis of the chromophores, illustrated in Scheme 1, is strongly based on the Suzuki coupling reaction of commercially available materials.³¹ Suzuki coupling was carried out with unprotected 5-formyl-2-thiophene-boronic acid and 4-(diphenylamino)-bromobenzene under microwave irradiation to directly yield the aldehyde in **1**, necessary in the final reactions. Bromination of the *para*-positions of the triphenylamine moiety was carried out with NBS to yield **2**. Additional Suzuki coupling reactions under microwave irradiation introduced the functionalized phenyl groups. The final reaction of the three dyes was the condensation of the respective aldehydes with cyanoacetic acid by the Knoevenagel reaction in presence of piperidine.

Table 1 presents the experimental spectral and electrochemical properties of the dyes in ethanol solution and adsorbed onto TiO₂, respectively. The predicted red-shift in the absorption maxima, due to the increasing electron-donating strength of the moieties, was observed. As seen in Fig. 4, the difference is small, and the theoretical overestimation of absorption wavelength is evident. In the experimental spectrum for **D37**, a slight broadening at the blue end of the visible band is observed. We believe that this is due to the second transition discussed above. The appearance of only one band can be explained by solvation broadening and the fact that the two vertical transitions are closer in reality than in the theoretical spectrum, thus embedded



Scheme 1 Synthesis of the chromophores.

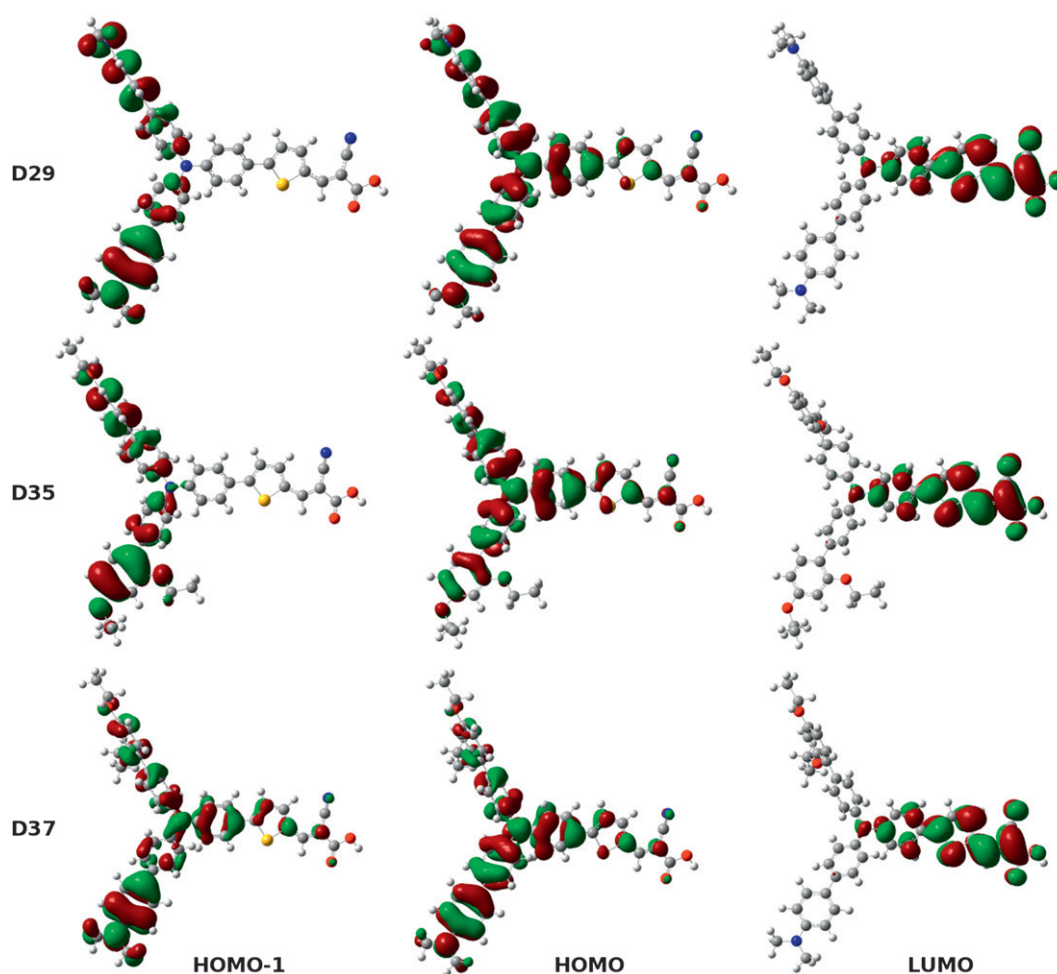


Fig. 2 Isodensity plots of the new organic chromophores, showing HOMO-1, HOMO and LUMO. Good charge separation is obtained by transferring an electron from an occupied orbital to the LUMO, facilitating electron injection. **D37** is the only of the three dyes where the HOMO-1 orbital extends over the linker region, which explains the relatively strong second transition. Note that the butoxy groups have been truncated in the calculations, in order to save computational time. This does not significantly affect the electronic or spectral properties.

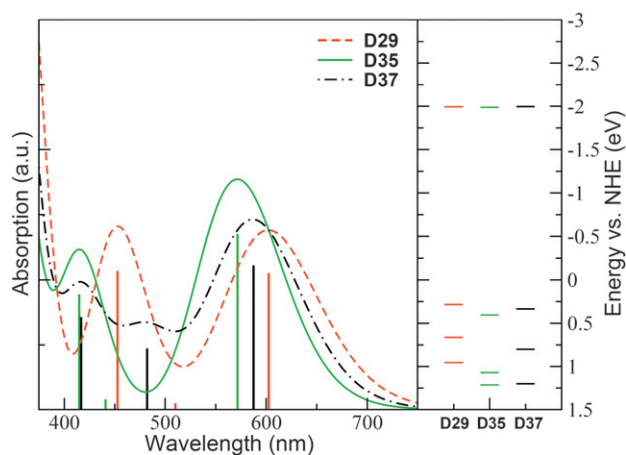


Fig. 3 Calculated gas-phase absorption spectra of the sensitizers. Each spectrum was generated by employing an arbitrary Gaussian broadening of 3000 cm^{-1} , and the calculated transitions are shown as vertical lines. The right panel shows relative energy levels.

in the same band. The estimated LUMO energy levels, calculated from $E_{(\text{HOMO}_{0\text{x}})} - E_{0-0}$, seem to be sufficiently more negative than the TiO_2 conduction-band edge for all three dyes, reported in Table 1.

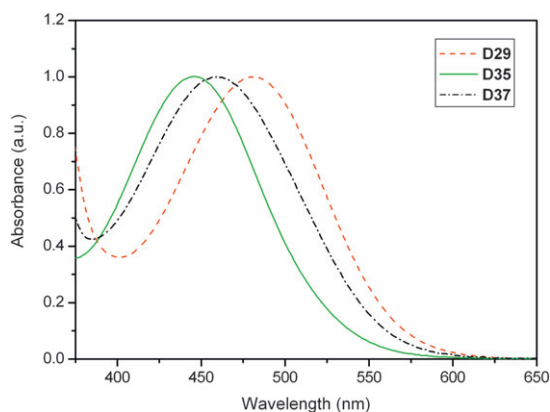
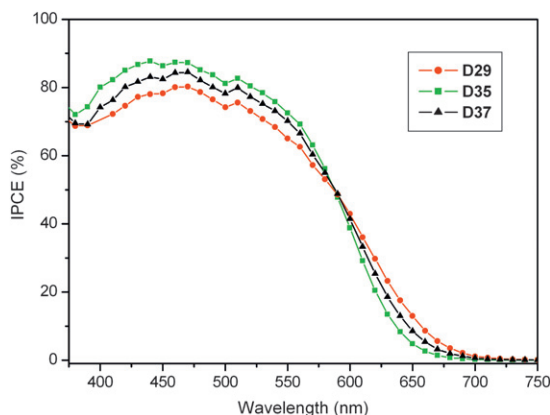
However, the LUMO energy level of **D37** is surprisingly negative, and not at all in the same region as the two parent chromophores, **D29** and **D35**, which was predicted. The monochromatic IPCE spectra are presented in Fig. 5, and show that the highest IPCE is obtained from the **D35** solar cell. The IPCE of **D37** is a combination of the two parent chromophores, but not quite as red as the **D29** nor as high as the **D35**. A comparison of the photovoltaic performances of solar cells based on the different dyes **D29**, **D35** and **D37** under AM 1.5 illumination is presented in Table 2. The efficiencies were 4.83, 6.00 and 5.24% for **D29**, **D35** and **D37**, respectively.

The **D35** dye showed remarkably high V_{oc} , 0.75 V, which we believe is due to an insulating effect of the bulky butoxy chains.¹⁷ This is also supported by our preliminary electron-lifetime studies, which are presented in Fig. 6. Comparing the electron

Table 1 Experimental data for the spectral and electrochemical properties of the dyes

Dye	Abs _{max} /nm ^a	ϵ /M ⁻¹ cm ⁻¹	Em _{max} /nm	$E_{(\text{HOMO}_{\text{ox}})/V^b}$ vs. NHE	E_{0-0}/eV^c (Abs/Em)	$E_{(\text{LUMO})/V^d}$ vs. NHE
D29	482 ⁱ , 456 ⁱⁱ	70 200	612	0.84	2.31	-1.47
D35	445 ⁱ , 444 ⁱⁱ	70 100	597	1.04	2.41	-1.37
D37	459 ⁱ , 446 ⁱⁱ	37 200	576	0.81	2.41	-1.6

^a Absorption of the dyes in EtOH solutionⁱ and adsorbed onto TiO₂ⁱⁱ. ^b The ground-state oxidation potential of the dyes was measured under the following conditions: Pt working electrode and Pt counter electrode; electrolyte, 0.05 M tetrabutylammonium hexafluorophosphate, TBA(PF₆), in DMF. Potentials measured vs. Fc^{+/0} were converted to normal hydrogen electrode (NHE) by addition of +0.63 V. ^c 0–0 transition energy, estimated from the intercept of the normalized absorption and emission spectra in ethanol. ^d Estimated LUMO energies vs. NHE from the estimated highest-occupied molecular orbital (HOMO) energies obtained from the ground-state oxidation potential, $E_{(\text{HOMO}_{\text{ox}})}$, by subtracting the 0–0 transition energy, E_{0-0} .

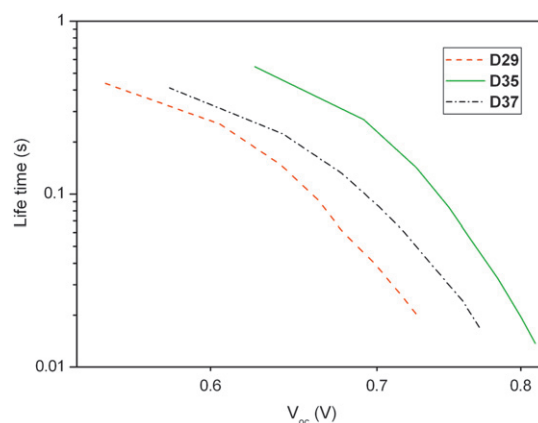
**Fig. 4** Normalized absorption spectra of **D29** (red), **D35** (green), and **D37** (black line) measured in ethanol.**Fig. 5** Spectra of incident photon-to-current conversion efficiency (IPCE) for DSCs based on **D29**, **D35**, and **D37** dyes.

lifetimes as a function of V_{oc} , DSCs based on **D35** showed significantly longer electron lifetimes compared to **D37** and **D29**. This provides support for the four insulating butoxy chains introduced in **D35** preventing electrons in TiO₂ from recombining with redox species yielding a high V_{oc} . Despite the red-shift in the absorption spectrum and hence a more optimal HOMO and LUMO energy-level composition with regards to the TiO₂-I⁻/I₃⁻ system, the **D29** dye showed a comparatively low performance due to the lack of insulating bulky substituents. The predicted broader spectral response of **D37** was not decisive for the

Table 2 Current and voltage characteristics of DSCs^a

Dye	V_{oc}/V	$J_{\text{sc}}/\text{mA cm}^{-2}$	ff	η (%)
D29 ^b	0.67	12.00	0.60	4.83
D35 ^c	0.75	12.96	0.61	6.00
D37 ^b	0.71	12.50	0.59	5.24

^a Photovoltaic performance under AM 1.5 irradiation of DSCs based on **D29**, **D35**, and **D37** dyes, respectively, based on 0.6 M tetrabutylammonium iodide (TBAI), 0.1 M LiI, 0.05 M I₂, 0.5 M 4-*tert*-butylpyridine (4-TBP), 0.05 M guanidinium thiocyanate (GuSCN) in acetonitrile. ^b Dye bath: acetonitrile solution (2×10^{-4} M) with addition of CDCA (6×10^{-3} M). ^c Dye bath: ethanol solution (2×10^{-4} M) with addition of CDCA (6×10^{-3} M).

**Fig. 6** Electron lifetime as a function of extracted charge under open-circuit conditions for DSCs based on **D29**, **D35**, and **D37**, respectively.

photovoltaic performance. We are currently working on the synthesis of spectrally and structurally benefited chromophores.

Conclusions

In conclusion, this series of chromophores showing high efficiencies in DSCs were used in a comparative study of structural *versus* spectral benefits. The TPA donor units were functionalized with electron-donating groups and bulky substituents, respectively. Neither the red-shift of the symmetrical dye **D29** nor the expanded spectral response from the unsymmetrical dye **D37** can compete with the structural benefits of the symmetrical dye **D35**. In the present study, solar cells based on **D35** yielded the

highest efficiency, thereby showing that structural properties are of central importance to solar cell efficiency.

Experimental section

General procedure for preparation of solar cells

Fluorine-doped tin oxide (FTO) glass plates (Pilkington-TEC8) were cleaned using (in order) detergent solution, water and ethanol using an ultrasonic bath overnight. The conducting glass substrates were immersed in 40 mM aqueous TiCl_4 solution at 70 °C for 30 min and washed with water and ethanol. The screen-printing procedure was repeated (layers of $\sim 3 \mu\text{m}$) with TiO_2 paste to obtain a transparent nanocrystalline film of thickness around 10 μm . The preparation of TiO_2 paste ($\sim 25 \text{ nm}$ colloidal particles) is described elsewhere.³² A scattering layer ($\sim 3 \mu\text{m}$, PST-400C, JGC Catalysts and Chemicals LTD) was deposited and a final thickness of $13.0 \pm 0.2 \mu\text{m}$ was attained. The TiO_2 electrodes were gradually heated in an oven (Nabertherm Controller P320) in an air atmosphere. The temperature gradient program had four levels at 180 °C (10 min), 320 °C (10 min), 390 °C (10 min) and 500 °C (60 min). After sintering, the electrodes once again passed, as described above, a post- TiCl_4 treatment. A second and final sintering, at 500 °C for 30 min, was performed. When the temperature decreased to 70 °C after the sintering, the electrodes were immersed into 0.2 mM dye solutions and kept for 16–17 h in darkness at room temperature. The solvent was ethanol (99.5%) for **D35**, acetonitrile (99.8%) for **D29** and **D37**, respectively. After the adsorption of the dyes, the electrode was rinsed with the same solvent. The electrodes were assembled with a platinized counter electrode using a hot-melt Surllyn film. The redox electrolyte consisted of 0.1 M LiI (99.9%), 0.6 M TBAI (98%), 0.05 M I_2 (99.9%), 0.5 M 4-TBP (99%), and 0.05 M GuSCN in acetonitrile (99.8%) was introduced through a hole drilled in the back of the counter electrode. Finally, the hole was also sealed with Surllyn film.

Photocurrent density–voltage (J – V) measurements.

The current–voltage characteristics and incident photon-to-current conversion efficiencies (IPCEs) of the prepared solar cells were studied. Current–voltage measurements were carried out with a Newport Oriel 300 W Solar Simulator (Model 91160) with AM 1.5 G filter. The incident light intensity was 1000 W m^{-2} calibrated with a standard Si solar cell. For the J – V curves, the solar cells were evaluated by using a slightly larger black mask (working area 0.25 cm^2 , aperture area of 0.49 cm^2) on the cell surface to avoid diffusive light. IPCE measurements were carried out with a Xenon arc lamp (300 W), a 1/8 m monochromator, a source/meter, and a power meter with a 818-UV detector head.

Photophysical measurements

All UV–vis spectra of dye solutions ($1 \times 10^{-5} \text{ M}$ in ethanol) were recorded on a Lambda 750 spectrophotometer using a 1 cm cuvette. All fluorescence spectra were recorded on a Cary Eclipse fluorescence spectrophotometer.

Electrochemical measurements

Electrochemical experiments were performed with a CH Instruments electrochemical workstation (model 660A) using a conventional three-electrode electrochemical cell. The supporting electrolyte consisted of 0.05 M TBAPF₆ in DMF and dye concentrations of $1 \times 10^{-3} \text{ M}$. A glass carbon disk was used as the working electrode, a platinum wire served as a counter electrode, a Ag/Ag⁺ electrode was utilized as a reference electrode, and the scan rate was 100 mV s^{-1} . All potentials were calibrated vs. a normal hydrogen electrode (NHE) by the addition of ferrocene as an internal standard taking $E^\circ(\text{Fc}/\text{Fc}^+) = 630 \text{ mV vs. NHE}$.

Electron-lifetime measurements

Electron lifetimes in the complete dye sensitized solar cell device were measured in a system using a red-light-emitting diode (Luxeon Star 1 W, $\lambda_{\text{max}} = 640 \text{ nm}$) as light source. Voltage traces were recorded using a 16-bit resolution data acquisition board (DAQ National Instruments) in combination with a current amplifier (Stanford Research Systems SR570) and a custom-made system using electromagnetic relay switches. Electron lifetimes were determined by monitoring the transient voltage responses after a small light intensity modulation (square-wave modulation, <10% intensity of 0.5 Hz), and the step response was recorded by the DAQ board. The voltage response was well fitted to first-order decay, and time constants were thus obtained.

General synthetic procedure

¹H and ¹³C NMR spectra were recorded on Bruker 500 and 400 MHz instruments by using the residual signals $\delta = 7.26 \text{ ppm}$ and 77.0 ppm from CDCl_3 , $\delta = 2.50$ and 39.4 ppm from $[\text{D}_6]\text{-DMSO}$ and $\delta = 2.05$, 29.84, and 206.26 ppm from $[\text{D}_6]\text{-acetone}$, as internal references for ¹H and ¹³C respectively. HRMS was performed using a Q-ToF Micro (Micromass Inc., Manchester, England) mass spectrometer equipped with a Z-spray ionization source.

5-(4-(Diphenylamino)phenyl)thiophene-2-carbaldehyde (1). The synthetic procedure and characterizations were presented in an earlier publication.²³

5-(4-(Bis(4-bromophenyl)amino)phenyl)thiophene-2-carbaldehyde (2). **1** (400 mg, 1.13 mmol) was dissolved in THF (50 mL) and the solution was cooled to 0 °C. NBS (411 mg, 2.31 mmol) was added in one portion and the mixture was stirred for 1 h at 0 °C. The mixture was allowed to warm to ambient temperature and stirring was continued for 1.5 h. The reaction was quenched by addition of water (50 mL), extracted with diethyl ether (50 mL), washed with water ($3 \times 50 \text{ mL}$) and purified by filtration through a plug of silica gel with DCM. Solvent removal by rotary evaporation yielded **2** as a yellow solid (577 mg, 100%). ¹H NMR (500 MHz, CDCl_3) δ ppm 9.86 (s, 1H), 7.71 (d, $J = 3.9 \text{ Hz}$, 1H), 7.54 (d, $J = 8.7 \text{ Hz}$, 2H), 7.39 (d, $J = 8.8 \text{ Hz}$, 4H), 7.32 (d, $J = 4.0 \text{ Hz}$, 1H), 7.06 (d, $J = 8.7 \text{ Hz}$, 2H), 6.99 (d, $J = 5.8 \text{ Hz}$, 4H); ¹³C NMR (126 MHz, CDCl_3) δ ppm 182.6, 153.9, 148.0, 145.7, 141.7, 137.6, 132.6, 127.5, 127.4, 126.2, 123.27, 123.2, 116.7.

5-(4-(Bis(4'-(dimethylamino)biphenyl-4-yl)amino)phenyl)thiophene-2-carbaldehyde (5a). **2** (200 mg, 390 μmol), 4-(dimethylamino)phenylboronic acid (142 mg, 857 μmol), K_2CO_3 (269 mg, 1.95 mmol) and $\text{PdCl}_2(\text{dppf})$ (31.8 mg, 39 μmol) was added to a mixture of DCM and methanol (3:2, 5 mL). The mixture was heated by microwave irradiation to 70 $^\circ\text{C}$ for 20 min. The reaction was quenched by the addition of water (20 mL) and extracted with DCM (2 \times 30 mL). The combined extracts were dried over anhydrous MgSO_4 and filtered. Solvent removal by rotary evaporation followed by column chromatography over silica gel with DCM yielded **5a** as an orange solid (165 mg, 71%). ^1H NMR (500 MHz, CDCl_3) δ ppm 9.86 (s, 1H), 7.71 (d, $J = 4.0$ Hz, 1H), 7.54 (d, $J = 8.7$ Hz, 2H), 7.50 (d, $J = 8.6$ Hz, 8H), 7.31 (d, $J = 4.0$ Hz, 1H), 7.20 (d, $J = 8.5$ Hz, 4H), 7.14 (d, $J = 8.7$ Hz, 2H), 6.81 (d, $J = 8.8$ Hz, 4H), 3.00 (s, 12H); ^{13}C NMR (126 MHz, CDCl_3) δ ppm 182.5, 154.7, 149.8, 149.1, 144.9, 141.1, 137.7, 136.7, 128.4, 127.3, 127.2, 127.0, 125.7, 125.4, 122.7, 122.0, 112.7, 40.5; HRMS (TOF-MS-ESI) m/z : 593.2474 [M $^+$]; calcd for $\text{C}_{39}\text{H}_{35}\text{N}_3\text{OS}$ [M $^+$]: 593.2495.

(E)-3-(5-(4-(Bis(4'-(dimethylamino)biphenyl-4-yl)amino)phenyl)thiophen-2-yl)-2-cyanoacrylic acid (D29). A 50 mL acetonitrile solution of **5a** (110 mg, 185 μmol) and cyanoacetic acid (18.9 mg, 476 μmol) for 4 h. The solvent was removed by rotary evaporation. The product was purified by chromatography over silica gel (short column) using a DCM to DCM–methanol (9 : 1) gradient and washed with a 1 M HCl solution upon which the product precipitated. The precipitate was dissolved in methanol which was removed by rotary evaporation to yield **D29** (87 mg, 71%) as a dark-red solid. ^1H NMR (500 MHz, $[\text{D}_6]\text{-DMSO}$) δ ppm 8.47 (s, 1H), 8.00 (m, 1H), 7.73 (m, 6H), 7.66 (m, 5H), 7.50 (s, 4H), 7.18 (d, $J = 8.3$ Hz, 4H), 7.10 (d, $J = 8.4$ Hz, 2H), 3.08 (s, 12H); ^{13}C NMR (126 MHz, $[\text{D}_6]\text{-DMSO}$) δ ppm 163.7, 153.0, 148.1, 146.6, 145.4, 141.7, 134.7, 134.6, 133.6, 127.6, 127.5, 127.4, 127.4, 126.0, 125.0, 124.2, 122.6, 118.3, 116.5, 97.3, 43.5; HRMS (TOF-MS-ESI) m/z : 660.2562 [M $^+$]; calcd for $\text{C}_{42}\text{H}_{36}\text{N}_4\text{O}_2\text{S}$ [M $^+$]: 660.2553.

5-(4-(Bis(2',4'-dibutoxybiphenyl-4-yl)amino)phenyl)thiophene-2-carbaldehyde (5b), 5-(4-(2',4'-dibutoxybiphenyl-4-yl)(4'-(dimethylamino)biphenyl-4-yl)amino)phenyl)thiophene-2-carbaldehyde (5c). **2** (74 mg, 144 μmol), 2,4-dibutoxyphenylboronic acid (81 mg, 303 μmol), K_2CO_3 (100 mg, 721 μmol) and $\text{PdCl}_2(\text{dppf})$ was added to a mixture of DCM and methanol (3 : 2, 3 mL). The mixture was heated by microwave irradiation to 60 $^\circ\text{C}$ for 30 min. The reaction was quenched by addition of 10 mL water and extracted with DCM (2 \times 20 mL). Solvent removal by rotary evaporation followed by column chromatography over silica gel with ethyl acetate–pentane (1 : 5) yielded a crude intermediate (88 mg). The crude intermediate was added to a mixture of toluene and methanol (3:2, 3 mL) together with 4-(dimethylamino)phenylboronic acid (56.6 mg, 342 μmol), K_2CO_3 (118 mg, 855 μmol) and $\text{PdCl}_2(\text{dppf})$ (14 mg, 17 μmol). The mixture was heated by microwave irradiation to 70 $^\circ\text{C}$ for 20 min. The reaction was quenched by addition of water (20 mL) and extracted with DCM (2 \times 20 mL). Solvent removal by rotary evaporation followed by column chromatography over silica gel using a DCM–pentane 1 : 1 to DCM–methanol 9 : 1 gradient and yielded **5b** (35 mg, 30%) as a yellow solid; ^1H NMR (500 MHz,

CDCl_3) δ ppm 9.86 (s, 1H), 7.71 (d, $J = 4.0$ Hz, 1H), 7.54 (d, $J = 8.8$ Hz, 2H), 7.48 (d, $J = 8.6$ Hz, 4H), 7.31 (d, $J = 4.0$ Hz, 1H), 7.28 – 7.25 (m, 2H), 7.21 – 7.15 (m, 6H), 6.57 – 6.53 (m, 4H), 4.02 – 3.95 (m, 8H), 1.81 – 1.72 (m, 8H), 1.55 – 1.49 (m, 4H), 1.45 – 1.41 (m, 4H), 1.00 (t, $J = 7.4$, 7.4 Hz, 6H), 0.94 (t, $J = 7.4$, 7.4 Hz, 6H); ^{13}C NMR (126 MHz, CDCl_3) δ ppm 182.5, 159.6, 156.9, 154.8, 149.2, 145.0, 141.1, 137.7, 133.9, 130.8, 130.3, 127.1, 125.8, 124.4, 122.8, 122.7, 122.3, 105.3, 100.4, 68.1, 67.7, 31.3, 31.1, 19.3, 19.2, 13.8, 13.8; HRMS (TOF-MS-ESI) m/z : 795.3959 [M $^+$]; calcd for $\text{C}_{51}\text{H}_{57}\text{NO}_5\text{S}$ [M $^+$]: 795.3952 and **5c** (22 mg, 22%) as an orange solid; ^1H NMR (500 MHz, $[\text{D}_6]\text{-acetone}$) δ ppm 9.88 (s, 1H), 7.90 (d, $J = 4.0$ Hz, 1H), 7.67 (d, $J = 8.7$ Hz, 2H), 7.57 (d, $J = 8.6$ Hz, 2H), 7.52 (m, 5H), 7.25 (d, $J = 8.4$ Hz, 1H), 7.16 (m, 4H), 7.09 (d, $J = 8.7$ Hz, 2H), 6.80 (d, $J = 8.8$ Hz, 2H), 6.61 (d, $J = 2.3$ Hz, 1H), 6.57 (dd, $J = 8.4$, 2.3 Hz, 1H), 4.00 (m, 4H), 2.95 (s, 6H), 1.71 (m, 4H), 1.45 (m, 4H), 0.95 (t, $J = 7.4$, 7.4 Hz, 3H), 0.89 (t, $J = 7.4$, 7.4 Hz, 3H); ^{13}C NMR (126 MHz, $[\text{D}_6]\text{-acetone}$) δ ppm 182.6, 159.7, 156.9, 154.8, 149.8, 149.2, 145.0, 141.1, 137.7, 136.8, 134.0, 130.8, 130.4, 128.5, 127.3, 127.2, 127.1, 125.8, 125.5, 124.4, 122.8, 122.7, 122.2, 112.8, 105.3, 100.5, 68.2, 67.8, 40.6, 31.4, 31.2, 19.4, 19.29, 13.9, 13.8; HRMS (TOF-MS-ESI) m/z : 694.3223 [M $^+$]; calcd for $\text{C}_{45}\text{H}_{46}\text{N}_2\text{O}_3\text{S}$ [M $^+$]: 694.3224.

(E)-3-(5-(4-(Bis(2',4'-dibutoxybiphenyl-4-yl)amino)phenyl)thiophen-2-yl)-2-cyanoacrylic acid (D35). A 10 mL acetonitrile solution of **5b** (75 mg, 94 μmol) and cyanoacetic acid (9.62 mg, 113 μmol) was refluxed in the presence of piperidine (27 mg, 317 μmol) for 24 h. Additional cyanoacetic acid (10 mg, 117 μmol) and piperidine (27 mg, 317 μmol) was added and reflux continued for 3 h. The temperature was reduced to 50 $^\circ\text{C}$ and stirring continued for 40 h. The solvent was removed by rotary evaporation and the product purified by chromatography over silica gel (short column) using a DCM to DCM–methanol (9 : 1) gradient. The solvent was removed by rotary evaporation. The product was dissolved in DCM (20 mL) and washed with 1 M HCl (2 \times 20 mL) and the solvent was removed by rotary evaporation to finally yield **D35** (70 mg, 86%) as a red solid. ^1H NMR (500 MHz, $[\text{D}_6]\text{-DMSO}$) δ ppm 8.45 (s, 1H), 7.98 (d, $J = 4.1$ Hz, 1H), 7.69 (d, $J = 8.7$ Hz, 2H), 7.64 (d, $J = 4.0$ Hz, 1H), 7.47 (d, $J = 8.5$ Hz, 4H), 7.23 (d, $J = 8.4$ Hz, 2H), 7.11 (d, $J = 8.5$ Hz, 4H), 7.05 (d, $J = 8.7$ Hz, 2H), 6.62 (d, $J = 1.9$ Hz, 2H), 6.58 (dd, $J = 8.5$, 2.0 Hz, 2H), 4.02 – 3.95 (m, 8H), 1.73 – 1.60 (m, 8H), 1.45 (dd, $J = 14.9$, 7.4 Hz, 4H), 1.39 – 1.34 (m, 4H), 0.94 (t, $J = 7.4$, 7.4 Hz, 6H), 0.87 (t, $J = 7.4$, 7.4 Hz, 6H); ^{13}C NMR (126 MHz, $[\text{D}_6]\text{-DMSO}$) δ ppm 163.6, 159.2, 156.4, 148.5, 144.2, 133.7, 133.4, 131.4, 130.4, 130.1, 128.5, 127.3, 125.2, 124.1, 123.8, 121.7, 121.5, 116.6, 105.8, 100.1, 67.5, 67.1, 30.7, 30.5, 18.7, 18.6, 13.6, 13.5; HRMS (TOF-MS-ESI) m/z : 861.3956 [M $^-$]; calcd for $\text{C}_{54}\text{H}_{57}\text{N}_2\text{O}_6\text{S}$ [M $^-$]: 861.3943.

(E)-2-Cyano-3-(5-(4-(2',4'-dibutoxybiphenyl-4-yl)(4'-(dimethylamino)biphenyl-4-yl)amino)phenyl)thiophen-2-yl)acrylic acid (D37). A 10 mL acetonitrile solution of **5c** (23 mg, 33 μmol) and cyanoacetic acid (3.38 mg, 40 μmol) was refluxed in the presence of piperidine (27 mg, 317 μmol) for 4 h. The solvent was removed by rotary evaporation. The product was purified by chromatography over silica gel (short column) using a DCM to DCM–methanol (9 : 1) gradient. The solvent was removed by rotary evaporation, the product dissolved in DCM (20 mL) and washed with 1 M HCl

(2 × 20 mL). Removal of the solvent with rotary evaporation yielded **D37** (17 mg, 67%) as a dark red solid. ¹H NMR (500 MHz, [D₆]-DMSO) δ ppm 8.47 (s, 1H), 8.00 (d, *J* = 4.2 Hz, 1H), 7.71 (d, *J* = 8.7 Hz, 2H), 7.68 – 7.59 (m, 5H), 7.48 (d, *J* = 8.6 Hz, 2H), 7.24 (d, *J* = 8.4 Hz, 1H), 7.15 (t, *J* = 8.7, 8.5 Hz, 5H), 7.07 (d, *J* = 8.7 Hz, 2H), 6.63 (d, *J* = 2.2 Hz, 1H), 6.58 (dd, *J* = 8.5, 2.2 Hz, 1H), 4.03 – 3.95 (m, 4H), 3.02 (s, 6H), 1.75 – 1.61 (m, 4H), 1.50 – 1.32 (m, 4H), 0.95 (t, *J* = 7.4, 7.4 Hz, 3H), 0.88 (t, *J* = 7.4, 7.4 Hz, 3H); ¹³C NMR (126 MHz, [D₆]-DMSO) δ ppm 163.7, 159.3, 156.4, 153.2, 148.4, 146.6, 144.2, 141.7, 133.9, 133.4, 130.5, 130.2, 127.4, 127.0, 125.3, 125.1, 124.2, 123.9, 121.8, 121.6, 116.5, 105.9, 100.2, 97.1, 67.6, 67.1, 30.7, 30.6, 18.7, 18.7, 13.6, 13.6; HRMS (TOF-MS-ESI) *m/z*: 761.3289 [M⁺]; calcd for C₄₈H₄₇N₃O₄S [M⁺]: 761.3282.

Acknowledgements

We acknowledge the Swedish Research Council, K & A Wallenberg Foundation, the Swedish Energy Agency for financial support of this work.

References

- B. O'Regan and M. Gratzel, *Nature*, 1991, **353**, 737.
- M. K. Nazeeruddin, A. Kay, I. Rodicio, R. Humphry-Baker, E. Muller, P. Liska, N. Vlachopoulos and M. Gratzel, *J. Am. Chem. Soc.*, 1993, **115**, 6382.
- M. K. Nazeeruddin, S. M. Zakeeruddin, R. Humphry-Baker, M. Jirousek, P. Liska, N. Vlachopoulos, V. Shklover, C. H. Fisher and M. Gratzel, *Inorg. Chem.*, 1999, **38**, 6298.
- M. K. Nazeeruddin, P. Pechy, T. Renouard, S. M. Zakeeruddin, R. Humphry-Baker, P. Comte, P. Liska, L. Cevey, E. Costa, V. Shklover, L. Spiccia, G. B. Deacon, C. A. Bignozzi and M. Gratzel, *J. Am. Chem. Soc.*, 2001, **123**, 1613.
- T. Horiuchi, H. Miura, K. Sumioka and S. Uchida, *J. Am. Chem. Soc.*, 2004, **126**, 12218.
- Z.-S. Wang, N. Koumura, Y. Cui, M. Takahashi, H. Sekiguchi, A. Mori, T. Kubo, A. Furube and K. Hara, *Chem. Mater.*, 2008, **20**, 3993.
- N. Koumura, Z. S. Wang, S. Mori, M. Miyashita, E. Suzuki and K. Hara, *J. Am. Chem. Soc.*, 2006, **128**, 14256.
- S. Kim, J. K. Lee, S. O. Kang, J. Ko, J. H. Yum, S. Fantacci, F. De Angelis, D. Di Censo, M. K. Nazeeruddin and M. Gratzel, *J. Am. Chem. Soc.*, 2006, **128**, 16701.
- Z. S. Wang, Y. Cui, K. Hara, Y. Dan-oh, C. Kasada and A. Shinpo, *Adv. Mater.*, 2007, **19**, 1138.
- K. R. J. Thomas, Y.-C. Hsu, J. T. Lin, K.-M. Lee, K.-C. Ho, C.-H. Lai, Y.-M. Cheng and P.-T. Chou, *Chem. Mater.*, 2008, **20**, 1830.
- D. P. Hagberg, J.-H. Yum, H. Lee, F. De Angelis, T. Marinado, K. M. Karlsson, R. Humphry-Baker, L. Sun, A. Hagfeldt, M. Gratzel and Md. K. Nazeeruddin, *J. Am. Chem. Soc.*, 2008, **130**, 6259.
- S. Ito, H. Miura, S. Uchida, M. Takata, K. Sumioka, P. Liska, P. Comte, P. Pechy and M. Gratzel, *Chem. Commun.*, 2008, 5194.
- H. Qin, S. Wenger, M. Xu, X. Jing, P. Wang, S. M. Zakeeruddin and M. Gratzel, *J. Am. Chem. Soc.*, 2008, **130**, 9202.
- Z. Ning, Q. Zhang, W. Wu, H. Pei, B. Liu and H. Tian, *J. Org. Chem.*, 2008, **73**, 3791.
- D. Kuang, S. Uchida, R. Humphry-Baker, S. M. Zakeeruddin and M. Gratzel, *Angew. Chem., Int. Ed.*, 2008, **47**, 1923.
- H. Choi, C. Biak, S. O. Kang, J. Ko, M.-S. Kang, Md. K. Nazeeruddin and M. Gratzel, *Angew. Chem., Int. Ed.*, 2008, **47**, 327.
- J.-H. Yum, D. P. Hagberg, S.-J. Moon, K. M. Karlsson, T. Marinado, L. Sun, A. Hagfeldt, Md. K. Nazeeruddin and M. Gratzel, *Angew. Chem., Int. Ed.*, 2009, **48**, 1576.
- J. T. Lin, P.-C. Chen, Y.-S. Yen, Y.-C. Hsu, H.-H. Chou and M.-C. P. Yeh, *Org. Lett.*, 2009, **11**, 97.
- G. Zhang, H. Bala, Y. Cheng, D. Shi, X. Lv, Q. Yu and P. Wang, *Chem. Commun.*, 2009, 2198.
- L. Schmidt-Mende, U. Bach, R. Humphry-Baker, T. Horiuchi, H. Miura, S. Ito, S. Uchida and M. Gratzel, *Adv. Mater.*, 2005, **17**, 813.
- D. P. Hagberg, T. Edvinsson, T. Marinado, G. Boschloo, A. Hagfeldt and L. Sun, *Chem. Commun.*, 2006, 2245.
- T. Kitamura, M. Ikeda, K. Shigaki, T. Inoue, N. A. Andersson, X. Ai, T. Lian and S. Yanagida, *Chem. Mater.*, 2004, **16**, 1806.
- K. Hara, M. Kurashige, Y. Dah-oh, C. Kasada, A. Shinpo, S. Suga, K. Sayama and H. Arakawa, *New J. Chem.*, 2003, **27**, 783–785.
- D. P. Hagberg, T. Marinado, K. M. Karlsson, K. Nonomura, P. Qin, G. Boschloo, T. Brinck, A. Hagfeldt and L. Sun, *J. Org. Chem.*, 2007, **72**, 9550.
- Z. S. Wang, F. Y. Li, C. H. Huang, L. Wang, M. Wei, L. P. Jin and N. Q. Li, *J. Phys. Chem. B*, 2000, **104**, 9676.
- P. Qin, X.-C. Yang, R.-K. Chen, L. Sun, T. Marinado, T. Edvinsson, G. Boschloo and A. Hagfeldt, *J. Phys. Chem. C*, 2007, **111**, 1853.
- S. Alex, U. Santhosh and S. Das, *J. Photochem. Photobiol., A*, 2005, **172**, 63–71.
- P. Qin, H. Zhu, T. Edvinsson, G. Boschloo, A. Hagfeldt and L. Sun, *J. Am. Chem. Soc.*, 2008, **130**, 8570.
- M. J. Frisch *et al.*, *GAUSSIAN 03 (Revision C.02)*, Pittsburgh, 2003.
- A. Dreuw and M. Head-Gordon, *Chem. Rev.*, 2005, **105**, 4009.
- A. Suzuki and J. Organomet, *Chem.*, 1999, **576**, 147.
- P. Wang, S. M. Zakeeruddin, P. Comte, R. Charvet, R. Humphry-Baker and M. Gratzel, *J. Phys. Chem. B*, 2003, **107**, 14336.